Woodford OJ, Stachelek P, Ziessel R, Algoazy N, Knight JG, Harriman A.
End-to-end communication in a linear supermolecule with a BOPHY centre and: *N,N*-dimethylanilino-based terminals.
***New Journal of Chemistry* 2018, 42(7), 4835-4842.**

DOI link to article:

https://doi.org/10.1039/c7nj04654e

Date deposited:

11/05/2018

Embargo release date:

13 February 2019

End-to-End Communication in a Linear Supermolecule with a BOPHY Centre and N,N-Dimethylanilino-based Terminals

Owen J. Woodford,[a] Patrycja Stachelek,[a,†] Raymond Ziessel,[a] Nawaf Algoazy,[b] Julian G. Knight[b] and Anthony Harriman[a,*]

The recently introduced BOPHY (i.e., symmetrical bis(pyrrole-BF_2)) chromophore is a highly attractive building block for constructing linear molecules with extended π-conjugation running along the molecular backbone. In order to assess the level of electronic communication between the terminal groups in this type of supermolecule, we have examined selective protonation and oxidation of the bis-(N,N-dimethylanilino-styryl) derivative. The amino N atoms are separated by 22.6 Å via a conjugated pathway but there is no indication for through-bond electronic coupling. Instead, the disparate pK_A values and also reduction potentials found for one-electron oxidation of each aniline group are well explained in terms of very long-range electrostatic interactions. It is necessary, however, to allow for the effects of ion-pairing. As an interesting aside, it is shown that protonation can be achieved in a cast PMMA film by using a suitable photo-acid generator.

Introduction

A recurring theme in molecular photophysics concerns the delineation of the precise size of a chromophore. This fundamental property of molecular spectroscopy is a particular challenge for highly conjugated molecules,[1] bichromophores,[2] stacked molecular aggregates,[3] conducting polymers[4] and photonic crystals.[5] Experimental determination of the conjugation length of an organic molecule in solution is far from straightforward, even by electro-optical spectroscopy,[6] while computational studies are not so reliable for molecules susceptible to internal rotation or twisting. The conjugation length affects many molecular properties, including colour, radiative probability, dipole moment, solubility, polarizability, oscillator strength and reduction potential, and is therefore a critical parameter. As highly conjugated fluorescent dyes[7,8] absorbing and emitting in the red region become available it seems important to better understand how individual modules accrete into the final supermolecule. Here, we describe the properties of an extended dye molecule[9] with terminal electron-donating groups that push electron density towards the centre. The two nitrogen atoms are separated by 22.6 Å and the overall molecule is essentially linear but with rotatable groups. We seek to establish to what extent, if any, the two terminals are electronically coupled.

Similar molecules have been synthesized previously,[10] and used as prototypic pH indicators,[11] but these possess a V-shaped geometry where the terminals favour through-space interactions. It should also be noted that a closely related derivative bearing a single amino residue was reported[12] recently and shown to function as a pH probe in acidic solution. Indeed, the weakly emissive parent compound was converted into a strongly fluorescent dye on protonation with HCl in aqueous acetonitrile. An analogous derivative[13] bearing ferrocene-based terminals, with the metal centres being separated by 17.2 Å, displays intervalence charge-transfer characteristics on partial oxidation. This latter work is of direct relevance to the present system.

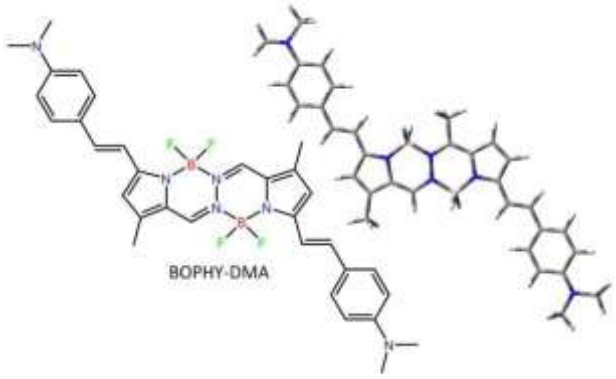

Figure 1. Molecular formula and energy-minimized geometry for the target compound, BOPHY-DMA, studied in this work.

Experimental

A sample of the target compound[9] (Figure 1) was available from earlier work and was used for all experimental studies reported here except for the near-infra-red absorption spectroscopy. For these latter studies only, a fresh sample was prepared following

[a] *Molecular Photonics Laboratory, School of Natural and Environmental Science, Bedson Building, Newcastle University, Newcastle upon Tyne, NE1 7RU, UK.*
[b] *School of Natural and Environmental Science, Bedson Building, Newcastle University, Newcastle upon Tyne, NE1 7RU, UK.*
†Present address: Department of Physics, Durham University, South Road, Durham DH1 3LE, UK.
Electronic Supplementary Information (ESI) available: [absorption spectrum in the region where the IVCT band is expected, computational data for calculation of pK_A, calculated HOMO/LUMO distributions, Lippert-Mataga plot].

the procedure reported earlier by Ziessel *et al*.[9] Solvents were spectroscopic grade, obtained from commercial sources, and checked for the presence of fluorescent impurities before use. Dichloromethane used for cyclic voltammetry studies was purchased as the anhydrous solvent for hplc and was freshly distilled over CaH_2 immediately before use. Anisole (methoxybenzene) was washed several times with aqueous NaOH (2M) to remove phenol residues, dried over $CaCl_2$, and passed down an alumina column. A sample was distilled from sodium before use. Titrations were carried out by dilution of stock solutions of HCl (2.5 M) in dioxane, the course of reaction being followed by absorption or emission spectroscopy. Data analysis was made with in-house software using well established algorithms.[14] The photo-acid[15] used was N-hydroxynaphthalimide triflate, as purchased from Sigma-Aldrich.

Absorption spectra were recorded with a Hitachi U-3310 spectrophotometer while fluorescence spectra were recorded with a Hitachi F-4500 spectrofluorimeter. All measurements were made at room temperature. Optically dilute solutions were used for the fluorescence measurements and quantum yields were determined[16] relative to Nile Blue in ethanol solution. Corrections[17] were made for changes in refractive index. Excited-singlet state lifetimes were measured by time-correlated single photon counting using laser excitation at 635 nm. Decay curves, after deconvolution with the instrument response function, could be analysed[18] satisfactorily in terms of single-exponential components. To monitor formation of the π-radical cation,[19] the target compound in aerated benzonitrile solution containing CCl_4 (ca. 1 M) was illuminated with white light (λ>350 nm) from a projector lamp for a few minutes. Absorption spectroscopy was used to follow the course of reaction. For near-IR studies, a Perkin-Elmer Lambda 950 spectrophotometer was used with spectra being recorded at wavelengths between 2500 and 500 nm.

Cyclic voltammetry was made with a CH Instruments potentiostat using a conventional 3-electrode set-up. The working electrode was a highly polished glassy carbon disc while the counter electrode was a Pt wire. The reference electrode was Ag/Ag^+ calibrated with respect to added ferrocene.[20] For these measurements, the concentration of solute was ca. 2 mM and the deaerated solution contained tetra-N-butyl ammonium tetrafluoroborate (0.2 M) as background electrolyte. A series of scan rates was used for all measurements.

Ground-state structure calculations were performed using the GAMESS program[21] with the PBE0 functional and the 6-311G(d,p) basis set. Energy-minimised structures were used for any subsequent calculation, with a background reservoir of chloroform molecules. The PCM solvent model[22] was applied with the Mennucci-Tomasi correction.[23] Partial atomic charges used to compute[24] pK_A values were calculated under the above conditions. Dipole moment calculations[25] were made using the PBE0 functional and the aug-cc-pVDZ basis set. Electrostatic interaction energies between the terminals at various states of electronic charge were calculated using MATLAB by applying the Kronecker product function. In all cases, reported geometries correspond to global minima. At least three different starting geometries were used and frequency calculations were carried out for all structures.

Results and Discussion

Spectroscopic properties in solution

Synthesis and characterisation of the target compound, abbreviated hereafter as BOPHY-DMA (Figure 1), was reported earlier.[9] The BOPHY unit is a close cousin of the well-known BODIPY family[26] of strongly fluorescent dyes and has the advantage of facile elongation of the molecular backbone. In benzonitrile solution, BOPHY-DMA exhibits a strong absorption transition (λ_{ABS}) centred at around 637 nm, with a molar absorption coefficient of ca. 90,000 M^{-1} cm^{-1} at the band maximum, together with weak fluorescence (λ_{FLU}) centred at ca. 730 nm (Figure 2). Under these conditions, the fluorescence quantum yield (Φ_F) has a value of 0.07 while the excited-state lifetime (τ_S) is 0.54 ns. Absorption is red-shifted relative to the parent dye[27] lacking the styryl residues (λ_{ABS} = 460 nm) because of the increased π-conjugation. An important point for this investigation concerns the realisation that the absorption maximum is considerably red-shifted compared to the corresponding mono-aminostyryl derivative[12] in a 1:1 mixture of acetonitrile and water (λ_{ABS} = 575 nm). This latter finding indicates extended π-electron delocalization running along the entire molecular backbone for BOPHY-DMA. It is the anticipation of this conjugation that suggests electronic coupling between the two terminals, despite their relatively large spatial isolation.

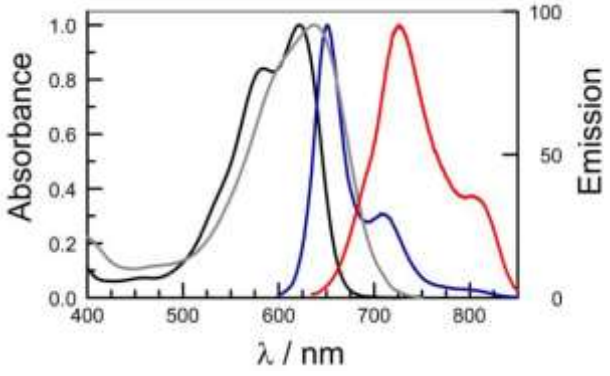

Figure 2. Absorption and fluorescence spectra recorded for BOPHY-DMA in cyclohexane (black and blue curves) and benzonitrile (grey and red curves) at room temperature.

The emission spectrum is also subject to a substantial red shift[28] and, due to intramolecular charge-transfer interactions involving the terminal groups, the Stokes' shift is considerably larger than that found for the parent dye. Indeed, the magnitude of the Stokes' shift increases linearly with the solvent Pekar function[29] (see Supporting Information) such that the change in dipole moment on excitation[30] can be estimated as being ca. 7.4 D. Quantum chemical calculations (DFT/PBE0/aug-cc-pVDZ/$CHCl_3$) indicate that the corresponding dipole moment for the ground state is 10.2 D. Similar

calculations (PCM/TD-DFT) give a dipole moment for the relaxed excited-singlet state of 18.5 D in $CHCl_3$. A combination of the red-shifted emission (i.e., lower excitation energy) and the intramolecular charge-transfer character (i.e., increased contribution from polar resonance structures) accounts for the reduced Φ_F value found in polar solvents. Indeed, both Φ_F and τ_S decrease in solvents of high polarity, as measured in terms of the dielectric constant or Pekar function. Such behaviour is fully consistent with that reported[10,11] for related amino-substituted BODIPY-based molecular probes. In the case of BOPHY-DMA, the fluorescence quantum yield falls from 80% in cyclohexane to less than 1% in acetonitrile solution. At the same time, the emission spectrum loses the fine structure seen in non-polar media and acquires the featureless, bell-shaped profile considered[31] characteristic of an intramolecular charge-transfer state (Figure 2). It is not the intention of the present study to dwell on the photophysical properties of BOPHY-DMA since several related BODIPY-based compounds are very well described[10,11,32] in the literature.

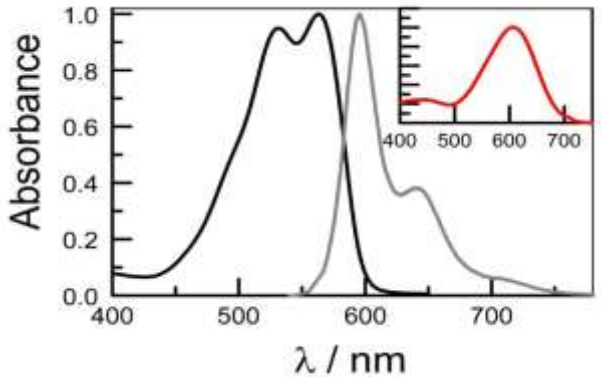

Figure 3. Absorption (black) and fluorescence (grey) spectra recorded for the diprotonated species in benzonitrile solution. The inset shows the absorption spectrum recorded for the corresponding mono-protonated species.

Protonation of the terminal amino groups

BOPHY-DMA, being terminated by aryl amino groups, provides the opportunity to use protonation to explore the extent of electronic coupling across the molecule. It is well known that protonation of chromophores can radically alter absorption/fluorescence energies and quantum yields. This was found to be the case for BOPHY-DMA where a solution in benzonitrile containing a slight excess of HCl was found to display an absorption maximum blue shifted by ca. 80 nm while the fluorescence quantum yield increased 10-fold from 6% to 60%. The solvent effects noted for the absorption and emission spectra of the neutral molecule are fully consistent with this species possessing a fair degree of intramolecular charge-transfer character. This impression is supported by the relatively broad absorption profile, the strongly red-shifted absorption maximum and the quantum chemical calculations. In contrast, the doubly protonated dye has significant π-π* character. This latter feature is evident from the structured absorption and emission profiles recorded in benzonitrile solution (Figure 3), although the Stokes' shift is larger than expected. The excited-singlet state lifetime measured under these conditions is 1.7 ns. Protonation serves to minimise the intramolecular charge-transfer character[33] and this effect accounts for the 80-nm blue shift. However, the molecule still retains extended conjugation relative to the parent compound and this effect pushes λ_{ABS} from 444 nm for the parent to 563 nm. The Stokes' shift (= 1,000 cm^{-1}) is greatly reduced for the diprotonated species, where the emission maximum is found at 596 nm in benzonitrile. The diprotonated species is unstable with respect to prolonged exposure to room light.[34]

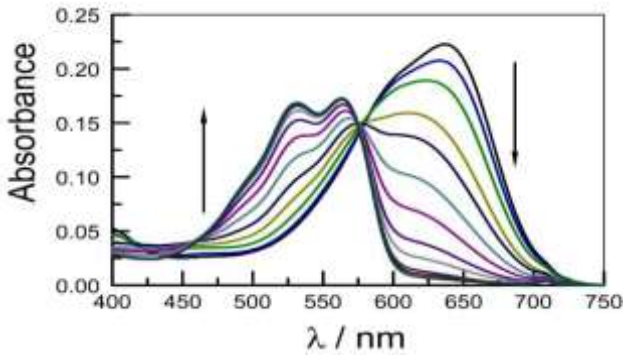

Figure 4. Absorption spectral profiles recorded during stepwise titration of the target compound with HCl in benzonitrile solution.

Stepwise addition of HCl causes evolution of the absorption and emission spectra from those of the neutral compound to the characteristic features assigned to the diprotonated species. During the titration, the presence of an intermediate, believed to be the monocation, can be resolved. Deconvolution[35] of the spectra of partially protonated solutions reveals the presence of a broad absorption profile centred at around 600 nm (Figure 3 insert). Absorbance due to this latter species increases during the early stages of the titration before decreasing as more acid is added (Figure 4). A Job plot[36] constructed for the monocationic intermediate is fully consistent with addition of a single proton to the neutral dye. As the titration continues, the monocation is converted quantitatively to the corresponding deprotonated species.

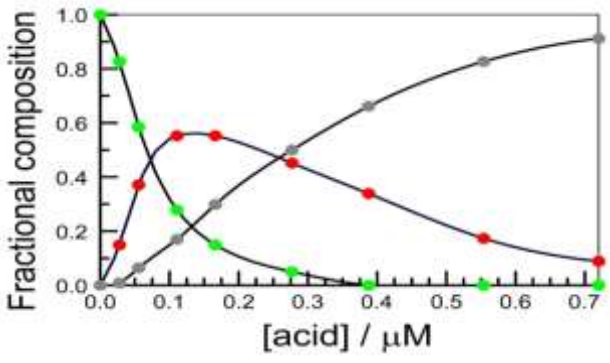

Figure 5. Evolution of the concentration changes during the titration of BOPHY-DMA with HCl in benzonitrile solution: neutral form (green), cationic species (red) and diprotonated species (grey).

A similar titration was made with the course of protonation being followed by fluorescence spectroscopy.[37] Here, the emission profile is set by the choice of excitation wavelength. Addition of acid causes loss of the weak fluorescence observed at long wavelength (λ_{FLU} = 730 nm) but there is no concomitant appearance of emission that might realistically be assigned to the cation. As more acid is added, the spectrum takes on the appearance of that already characterised for the diprotonated form of BOPHY-DMA (λ_{FLU} = 596 nm). The impression, therefore, is that the cation does not fluoresce with measurable yield within the wavelength range from 600 to 900 nm.

The acid dissociation constant is known for HCl in acetonitrile[38] at room temperature. Taking this value as being appropriate for benzonitrile, it is possible to analyse the spectroscopic titrations using standard statistical practices.[39] For the absorption data, successive pK_A values of 7.4 and 6.8 are derived for mono- and diprotonation of BOPHY-DMA under these conditions. The difference between the two pK_A values corresponds to 0.6 pH units. The evolution of the relative concentration gradient can be expressed by way of Figure 5, which emphasizes the growth and subsequent disappearance of the intermediate monocation.

Computational studies

The energy-minimized structures for the neutral, mono- and diprotonated forms of BOPHY-DMA were used as input data for calculation of their electronic properties. Calculated absorption maxima for neutral (λ_{ABS} = 661 nm; f = 1.04), cation (λ_{ABS} = 636 nm; f = 1.01) and dication (λ_{ABS} = 508; f = 1.47) species and oscillator strengths (f) are in fair agreement with experimental values. Using the computed partial atomic charge distributions for these species, together with those for simpler amines used as reference compounds,[24] it is possible to calculate pK_A values for BOPHY-DMA (see Supporting Information). The derived values are 7.3 and 6.8, which fall in excellent agreement with the experimental values.

A differential pK_A of 0.6 corresponds to an energy difference of ca. 35 mV. This can be compared to the electrostatic energy imposed by two positively charge spheres separated by 22.6 Å in a dielectric medium with ε_S of 26 (i.e., benzonitrile). The "theoretical" value so derived, which ignores the effects of ion pairing, is 25 mV. Again, agreement is reasonable. The computational studies are consistent with the major part of the partial atomic charge being localised at the amino N atom, thereby increasing the validity of the simple model used for the calculation. This electronic charge is not strictly embedded in a solvent reservoir, however, since the conjugated organic backbone disturbs the solvent structure. Taken literally, this comparison could indicate that addition of the second proton is more difficult than anticipated purely on the grounds of electrostatic repulsion. The actual difference is small, however.

Oxidation of the target compound in solution

A solution of BOPHY-DMA in aerated benzonitrile solution is stable over short illumination periods but degrades on longer timescales. Addition of carbon tetrachloride (ca. 1 M) followed by exposure to white light, however, causes rapid spectroscopic changes. Under these conditions, the trichloromethyl peroxyl radical[40] ($CCl_3OO^{\cdot}$) is formed (Scheme 1). This species is a powerful one-electron oxidant and oxidises the target compound to the π-radical cation (Figure 6). Over-exposure to light converts this intermediate species to the corresponding π-dication, which absorbs in the near-UV region. On the basis of quantum chemical calculation of the frontier molecular orbitals, oxidation should occur at one of the aniline groups but there is no suggestion that the oxidation equivalent will be localized at the nitrogen atom (see Supporting Information).

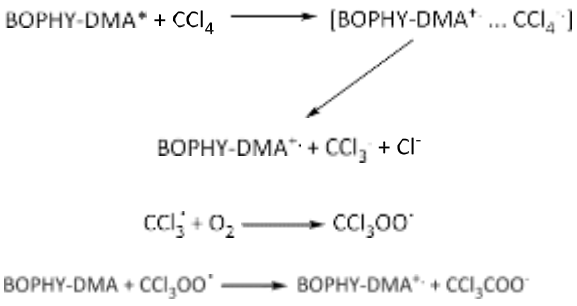

Scheme 1. Photooxidation of BOPHY-DMA to the π-radical cation using CCl_4 as electron-affinic reagent in benzonitrile solution.

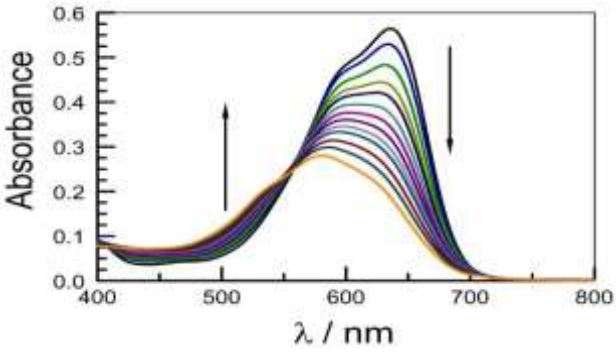

Figure 6. Progressive conversion of the neutral form of BOPHY-DMA to the π-radical cation under illumination in aerated benzonitrile in the presence of CCl_4.

The absorption spectrum recorded for the π-radical cation in benzonitrile solution comprises a broad and featureless band with a maximum at ca. 600 nm (Figure 6). The spectrum bears the hallmark[41] of an intramolecular charge-transfer transition. The electron density distribution for the SUMO is delocalised around one of the aniline-styryl units without penetrating onto the BOPHY nucleus (Figure 7). The two most likely transitions leading to the 600-nm absorption band involve promotion of an electron from the HOMO(-1) localised on the BOPHY core to the SUMO or promotion of the lone electron to the LUMO associated with the BOPHY nucleus. Both transitions correspond to intramolecular charge-transfer processes but the HOMO(-1) to SUMO transition (ΔE = 2.07 eV) gives the better match to the experimental energy of 2.0 eV.

In principle, the positive charge should alternate between the two terminal aniline groups, giving rise to a weak intervalence charge-transfer (IVCT) transition.[42] Such IVCT bands have been identified for π-radical cations formed from several somewhat related bis-amines[43] but the distance between the N atoms tends to be considerably less than the 22.6 Å found for BOPHY-DMA. The peak of the IVCT transition is usually seen in the far-red or near-IR spectral ranges. Unfortunately, it was not possible to detect an IVCT band for the π-radical cation derived from BOPHY-DMA at wavelengths less than 2500 nm. Because of the large separation between the N atoms, the electronic coupling matrix element characterising communication between the two terminals is likely to be small. According to Hush theory,[44] this will lower the molar absorption coefficient for the IVCT band, ensuring that detection is difficult.

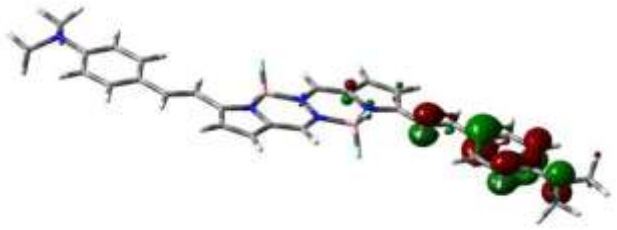

Figure 7. Kohn-Sham isodensity plot for the electron density distribution for the SUMO associated with the π-radical cation as produced by one-electron oxidation of BOPHY-DMA.

As a corollary to the above study, the target compound was studied by cyclic voltammetry in deoxygenated CH_2Cl_2 solution containing background electrolyte. An earlier study[9] showed one-electron reduction of the BOPHY residue with a half-wave potential of -1.28 V vs Ag/Ag^+ together with several overlapping oxidation waves at quite low potential. In our hands, one-electron reduction of BOPHY-DMA occurs with a half-wave potential of -1.31 V vs Ag/Ag^+. This process is *quasi*-reversible at fast scan rates but there appears to be some loss of the π-radical anion on slow scans. Compared to the parent BOPHY,[27] this reduction process occurs at relatively negative potentials which is considered to be further testimony to the intramolecular charge-transfer character inherent to this type of molecule. A second reduction step is seen at a peak potential of -2.0 V vs Ag/Ag^+. One-electron oxidation of the BOPHY unit can be identified with a peak potential of 1.05 V vs Ag/Ag^+ by reference to related BOPHY derivatives lacking the styryl arms.[9,25] This oxidation step is poorly reversible at all scan rates. The low potential region of the cyclic voltammograms corresponds to selective oxidation of the aniline residues. In dichloromethane at room temperature, this region contains two overlapping redox processes, with peak potentials of 0.48 and 0.575 V vs Ag/Ag^+ at modest (i.e., 150 mV/s) scan rates. These redox steps show limited reversibility, according to the scan rate.

Performing the cyclic voltammograms in deoxygenated anisole at low temperature (i.e., -70 ^{0}C in a dry ice/acetone mixture) leads to a significant increase in the reversibility of the low potential redox processes. The voltammogram is split into two *quasi*-reversible peaks with successive half-wave potentials of 0.39 and 0.32 V vs Ag/Ag^+ (Figure 8). The energy difference between these two redox steps is 70 mV, as measured at slow scan rate. This can be compared to the electrostatic energy that would arise from two point sources, each bearing a single positive charge and being separated by 22.6 Å, embedded in a reservoir of anisole molecules. This crude calculation requires knowledge of the static dielectric constant (ε_S) of anisole under the experimental conditions. Although there are reports[45] of a temperature effect for ε_S of anisole in mixtures with other solvents, these do not cover the range of interest here. Furthermore, the frontier molecular orbital calculations serve to show that the π-radical cation is not well represented by the point charge model. Rather, the electron density change on oxidation is distributed around the anilino-styryl unit, although the N atom is an important contributor. This shortens the distance between charges, thereby increasing the splitting energy caused by long-range electrostatic interactions relative to the protonation studies.

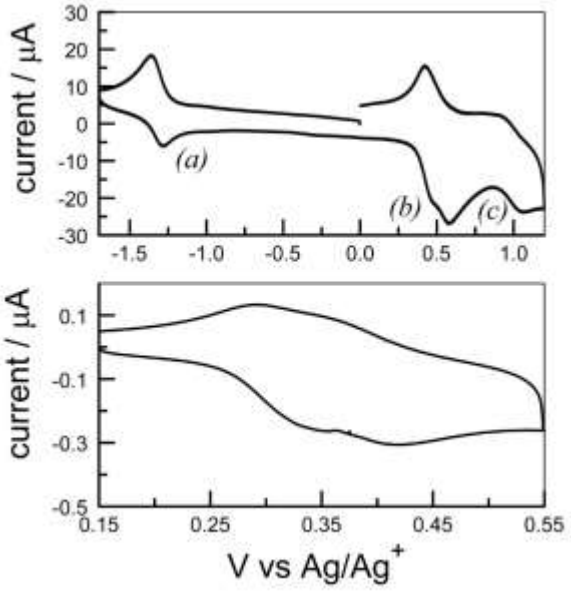

Figure 8. Examples of cyclic voltammograms recorded for BOPHY-DMA in CH_2Cl_2 at room temperature (upper panel) and anisole at -70 °C (lower panel). The lettering on the upper panel refers to (a) reduction of BOPHY, (b) oxidation of the aniline residues and (c) oxidation of BOPHY.

To estimate ε_S for anisole under our operating conditions, an indirect method was used whereby the fluorescence spectrum of a solvent-sensitive dye was recorded and calibrated by reference to a series of standard solvents at room temperature. The fluorescent sensor used was an 8-arylamino-BODIPY derivative[46] that displays exciplex emission in weakly polar solvents. From the fluorescence maximum, we conclude that the dielectric constant of the electrolyte solution at -80 ^{0}C is 6.1, compared to 4.3 for pure anisole[47] at room temperature.

Repeating the above calculation but replacing the point charges with atomic charges (i.e., the so-called atomistic approach[48]) leads to a refined electrostatic splitting energy of 108 mV. Thus, the experimental value of 70 mV is well below

the predicted result. Notably, for CH_2Cl_2 solution where the potential splitting between the successive aniline oxidation steps is 90 mV at slow (i.e., 40 mV/s) scan rates, the calculated value is 78 mV.

These apparent differences can be fully rationalised in terms of ion-pairing between the cation and the counterion. According to the Fuoss-Onsager equation,[49] this could be especially pronounced for the system in anisole at low temperature. Our results appear to be fully consistent with long-range electrostatic interactions mediated by the ion-pairing effect. In principle, it should be possible to perform calculations using an explicit anion to better simulate the effects of ion pairing but this is considered to be outside the scope of the present investigation.

Using a photo-acid generator

By judicious use of a photo-acid generator[50] (PAG) in a suitable solvent it becomes possible to drive the protonation of BOPHY-DMA by illumination with near-UV light. The photo-acid generator used was N-hydroxynaphthalimide triflate[15] in anisole solution, with activation at 365 nm. The subsequent optical spectra recorded for the protonated species remain in excellent agreement with those reported earlier. In itself, this observation is hardly surprisingly but the use of a PAG allows the acid/base changes to be realised in a solid device. For example, a thin PMMA film was cast from anisole to contain BOPHY-DMA and an excess of the PAG. The dried film was stable in the dark, although the PAG is a mild fluorescence quencher. Exposure of the film to near-UV light causes a colour change and the appearance of strong red fluorescence (Figure 9). This behaviour is fully consistent with photo-activated release of acid within the film and the ensuing protonation of the amino groups. The presence of molecular oxygen has no effect on the efficacy of this reaction.

Figure 9. Example of a cast film containing BOPHY-DMA and excess photo-acid generator, with half the film being exposed to near-UV light to allow formation of the red emitting diprotonated species.

One clear advantage of the film, relative to solution, relates to the capability to use a microscope fitted with a suitable LED to provide spatial resolution. High photon densities with focussed excitation leads directly to the diprotonated species and, because of the differential quantum yields and wavelength ranges, it is easy to visualise fluorescence from the doubly-protonated form even at low conversion. Used in conjunction with electronic energy transfer,[51] this type of reversible acid release could be used to fabricate intricate molecular-scale devices. It is also possible, although we did not attempt it here, to do complementary work with a photo-base.

Conclusions

This work has identified and quantified long-range electrostatic interactions between the charged terminals of the target compound following protonation or oxidation. The charges are associated with the aniline terminals but, in the case of one-electron oxidation, may be distributed around the terminal group. This leads to an effective fall in the separation distance because of the linear geometry. We have not been able to identify additional interactions, such as through-bond electronic coupling, and the overall magnitude of the electrostatic effects is kept modest by the wide separation. In particular, there is no evidence for the existence of an IVCT transition appearing in the far-red or near-infrared regions. Such optical transitions are invariably weak and difficult to resolve from the baseline but nonetheless the absence of the expected IVCT transition points to weak electronic communication along the molecular backbone.

In this context, it is interesting to recall that a closely related BOPHY derivative[13] bearing ferrocene units in place of the aniline groups reported that the BOPHY residue facilitated strong long-range metal-metal coupling. Indeed, the mixed-valence compound was reported to display an observable IVCT transition in the near-IR region. This situation is quite different from that described herein. All indications inform us that there is little, if any, through-bond electronic coupling between the terminals at the mono-cation stage. Electrostatic interactions cannot be ignored, however, even at such large separations.

Conflicts of interest

There are no conflicts to declare.

Acknowledgements

We are grateful to EPSRC (Industrial CASE Award to AH/OJW), the Saudi Arabian Cultural Bureau (King Abdullah Scholarship to JGK/NA) and Newcastle University for financial support of this work. We are indebted to Dr. Kumi-Barimah (University of Leeds) for providing access to the NIR spectrophotometer.

Notes and references

1 S. R. Marder, J. W. Perry, G. Bourhill, C. B. Gorman, B. G. Tiemann and K. Mansour, *Science*, 1993, **261**, 186.
2 P. Stachelek and A. Harriman, *J. Phys. Chem. A*, 2016, **120**, 8104.
3 M. Belletete, J. Bouchard, M. Leclerc and G. Durocher, *Macromolecules*, 2005, **38**, 880.
4 G. Klaerner and R. D. Miller, *Macromolecules*, 1998, **31**, 2007.
5 R. Al-Aqar, A. Atahan, A. C. Benniston, T. Perks, P. G. Waddell and A. Harriman, *Chem. Eur. J.*, 2016, **22**, 15420.
6 K. Nakagawa, S. Suzuki, R. Fujii, A. T. Gardiner, R. J. Cogdell, M. Nango and H. Hashimoto, *J. Phys. Chem. B,* 2008, **112**, 9467.
7 A. Abbotto, L. Beverina, R. Bozio, S. Bradamante, C. Ferrante, G. A. Pagani and R. Signorini, *Adv. Mater.*, 2000, **12**, 1963; P. Didier, G. Ulrich, Y. Mely and R. Ziessel, *Org. Biomol. Chem.*, 2009, **7**, 3639; Y. Gong, X. M. Guo, S. F. Wang, H. M. Su, A. D.

Xia, Q. G. He and F. L. Bai, *J. Phys. Chem. A*, 2007, **111**, 5806; M. Henary and A. Levitz, *Dyes Pigments*, 2013, **99**, 1107.
8 M. M. Oliva, J. Casado, M. M. M. Raposo, A. M. C. Fonseca, H. Hartmann, V. Hernandez and J. T. L. Navarrete, *J. Org. Chem*., 2006, **71**, 7509; S. Arzhantsev, K. A. Zachariasse and M. Maroncelli, *J. Phys. Chem. A*, 2006, **110**, 3454.
9 Q. Huaulme, A. Mirloup, P. Retailleau and R. Ziessel, *Org. Lett*., 2015, **17**, 2246.
10 R. Ziessel, P. Retailleau, K. J. Elliott and A. Harriman, *Chem. Eur. J*., 2009, **15**, 10369; C. Thivierge, J. Y. Han, R. M. Jenkins and K. Burgess, *J. Org. Chem*., 2011, **76**, 5219; S. Madhu, M. R. Rao, M. S. Shaikh and M. Ravikanth, *Inorg. Chem*., 2011, 50, 4392; K. Rurack, M. Kollmannsberger and J. Daub, *New J. Chem*., 2001, **25**, 289.
11 M. Z. Tian, X. J. Peng, F. Feng, S. M. Meng, J. L. Fan and S. G. Sun, *Dyes Pigments*, 2009, **81**, 58; L. Z. Gai, J. Mack, H. Lu, H. Yamada, D. Kuzuhara, G. Q. Lai, Z. F. Li and Z. Shen, *Chem. Eur. J*., 2014, **20**, 1091; N. Boens, V. Leen and W. Dehaen, *Chem. Soc. Rev*., 2012, **41**, 1130; M. Baruah, W. W. Qin, J. Hofkens, R. A. L. Vallee, D. Beljonne, M. Van der Aeweraer, W. M. De Borggraeve and N. Boens, *J. Phys. Chem. A*, 2006, **110**, 5998.
12 X. D. Jiang, Y. J. Su, S. Yue, C. Li, H. F. Yu, H. Zhang, C. L. Sun and L. J. Xiao, *RSC Adv*., 2015, **5**, 16735.
13 H. M. Rhoda, K. Chanawanno, A. J. King, Y. V. Zatsikha, C. J. Ziegler and V. N. Nemykin, *Chem. Eur. J*., 2015, **21**, 18043.
14 T. V. Parke and W. W. Davis, *Anal. Chem*., 1954, **26**, 642.
15 M. Saotome, S. Takano, A. Tokushima, S. Ito, S. Nakashima, Y. Nagasawa, T. Okada and H. Miyasaka, *Photochem. Photobiol. Sci*., 2005, **4**, 83.
16 R. Sens and K. H. Drexhage, *J. Lumin*., 1981, **24/25**, 709.
17 R. A. Lampert, S. R. Meech, J. Metcalfe, D. Phillips and A. P. Schaap, *Chem. Phys. Lett*., 1983, **94**, 137.
18 D. V. O'Connor and D. Phillips, Time-Correlated Single Photon Counting, Academic Press, London, 1984.
19 N. Carnieri and A. Harriman, *Inorg. Chim. Acta*, 1982, **62**, 103.
20 J. Zhang and A. M. Bond, *Anal. Chem*., 2003, **75**, 2694.
21 M. W. Schmidt, K. K. Baldridge, J. A. Boatz, S. T. Elbert, M. S. Gordon, J. H. Jensen, S. Koseki, N. Matsunaga, K. A. Nguyen, S. Su, T. L. Windus, M. Dupuis and J. A. Montgomery, *J. Comput. Chem*., 1993, **14**, 1347; M. S. Gordon, M. W. Schmidt, in "Theory and Applications of Computational Chemistry: the first forty years" C. E. Dykstra, G. Frenking, K. S. Kim, G. E. Scuseria (editors), Elsevier, Amsterdam, p. 1167, 2005.
22 B. Mennucci, J. Tomasi, R. Cammi, J. R. Chesseman, M. J. Frisch, F. J. Devlin, S. Gabriel and P. J. Stevens, *J. Phys. Chem. A*, 2002, **106**, 6102.
23 B. Mennucci and J. Tomasi, *J. Chem. Phys*., 1996, **106**, 5151.
24 C. L. Stanton and K. N. Houk, *J. Chem. Theory Comput*., 2008, **4**, 951.
25 A. L. Hickey and C. N. Rowley, *J. Phys. Chem. A*, 2014, **118**, 3678.
26 A. Loudet and K. Burgess, *Chem. Rev*., 2007, **107**, 4891; G. Ulrich, R. Ziessel and A. Harriman, *Angew. Chem., Int. Ed*., 2008, **47**, 1184; R. Ziessel, G. Ulrich and A. Harriman, *New J. Chem*., 2007, **31**, 496.
27 I. S. Tamgho, A. Hasheminasab, J. T. Engle, V. N. Nemykin and C. J. Ziegler, *J. Am. Chem. Soc*., 2014, **136**, 5623.
28 O. A. Kucherak, L. Richert, Y. Mely and A. S. Klymchenko, *Phys. Chem. Chem. Phys*., 2012, **14**, 2292; S. Sumalekshmy and K. R. Gopidas, *J. Phys. Chem. B*, 2004, **108**, 3705.
29 P. Suppan and N. Ghoneim, Solvatochromism, RSC, Cambridge, 1997.
30 E. Lippert, Z. *Naturforsch*, 1955, **10a**, 541; N. Mataga, Y. Kaifu and M. Koizumi, *Bull. Chem. Soc. Jpn*., 1956, **29**, 465.
31 M. Maus, W. Rettig, D. Bonafoux and R. Lapouyade, *J. Phys. Chem. A*, 1999, **103**, 3388.
32 T. Bura, P. Retailleau, G. Ulrich and R. Ziessel, *J. Org. Chem*., 2011, **76**, 1109.
33 A. Nano, P. Retailleau, J. P. Hagon, A. Harriman and R. Ziessel, *Phys. Chem. Chem. Phys*., 2014, **16**, 10187.
34 P. Stachelek, A. A. Alsimaree, R. B. Alnoman, A. Harriman and J. G. Knight, *J. Phys. Chem. A*, 2017, **121**, 2096.
35 N. Di Cesare and J. R. Lakowicz, *J. Photochem. Photobiol. A Chem*., 2001, **143**, 39.
36 J. S. Renny, L. L. Tomasevich, E. H. Tallmadge and D. B. Collum, *Angew. Chem., Int. Ed. Engl*., 2013, **52**, 11998.
37 J. M. Alvarez-Pez, L. Ballesteros, E. Talavera and J. Yguerabide, *J. Phys. Chem. A*, 2001, **105**, 6320.
38 E. Paenurk, K. Kaupmees, D. Himmel, A. Kutt, I. Kaljurand, I. A. Koppel, I. Krossing and I. Leito, *Chem. Sci*., 2017, **8**, 6964.
39 L. M. Schwartz and R. I. Gelb, *Anal. Sci*., 1978, **50**, 1571.
40 Z. B. Alfassi, A. Harriman, S. Mosseri and P. Neta, *Int. J. Chem. Kinetics*, 1986, **18**, 1315.
41 S. Barlow, C. Risko, S. J. Chung, N. M. Tucker, V. Coropceanu, S. C. Jones, Z. Levi, J. L. Bredas and S. R. Marder, *J. Am. Chem. Soc*., 2005, **127**, 16900.
42 D. M. D'Alessandro and F. R. Keene, *Chem. Soc. Rev*., 2006, **35**, 424.
43 B. He and O. S. Wenger, *J. Am. Chem. Soc*., 2011, **133**, 17027; R. Sakamoto, T. Sasaki, N. Honda and T. Yamamura, *Chem. Commun*., 2009, 5156; A. C. Jahnke, J. Proppe, M. Spulber, C. G. Palivan, C. Herrmann and O. S. Wenger, *J. Phys. Chem. A*, 2014, **118**, 11293.
44 J. Bonvoisin, J. P. Launay, C. Rovira and J. Veciana, *Angew. Chem., Int. Ed. Engl*., 1994, **33**, 2106.
45 G. E. Papanastasiou and I. I. Zlogas, *J. Chem. Eng. Data*, 1992, **37**, 187; G. E. Papanastasiou, A. D. Papoutsis and G. I. Kokkinidis, *J. Chem. Eng. Data*, 1987, **32**, 377.
46 S. Mula, K. Elliott, A. Harriman and R. Ziessel, *J. Phys. Chem. A*, 2010, **114**, 10515.
47 C. Wohlfarth, Dielectric constant of 1,4-dioxane. In Supplement to IV/6. Landolt-Börnstein – Group IV Physical Chemistry (Numerical Data and Functional Relationships in Science and Technology) Vol. 17, Springer, Berlin, 2008.
48 C. Li and T.-W. Chou, *App. Phys. Lett*., 2006, **89**, 063103.
49 J. C. Justice, *Electrochim. Acta*, 1971, **16**, 701.
50 G. Pohlers, J. C. Scaiano and R. Sinta, *Chem. Mater*., 1997, **9**, 3222.
51 D. Hablot, A. Harriman and R. Ziessel, *Angew. Chem., Int. Ed*., 2011, **50**, 7833.

Table of Contents Entry

Long-range electrostatic interactions are sufficient to cause sequential ionization of the terminal groups in a BOPHY-based supermolecule.